Breast Cancer Cell Adhesion Strength Following Lentivirus-Mediated Myoferlin Depletion

Undergraduate Honors Thesis

Presented in Partial Fulfillment of the Requirements for

Graduation with Distinction in Research

at The Ohio State University

By

Meagan Bechel

Undergraduate Program in Biomedical Engineering

The Ohio State University 2011

Thesis Committee:

Dr. Douglas Kniss, Advisor

Dr. Samir Ghadiali

Table of Contents

List of Figures

List of Tables

Abstract

The purpose of this project was to quantify the effect of lentiviral-based knockdown of myoferlin on the adhesion and spreading of MDA-MB-231 human breast cancer cells. Myoferlin was selected for this project because it is over expressed in metastatic breast cancer cells. While the effects of the gene knockdown on the morphology of MDA-MB-231 cells have been observed, it has yet to be analyzed in detail, and, thus, a cellular adhesion strength assay was developed. The cells were plated into xCELLigence E-plates and allowed to attach for 48 hr. The xCELLigenceE-Plate system measures the cells' relative adhesion strength, degree of spreading, and cell number by calculating the changing electrical resistance as a result of cellular interaction with gold electrodes at the bottom of the culture well. This measurement is reported as cellular index (CI). Initial spreading and adhesion measurements were taken from the first 3hrs of recordings. A difference in initial cell adhesion and spreading has been observed between the myoferlin-deficient and native cells, with the myoferlin-deficient cells having approximately twice the CI. After 48 hrs, trypsin (0.41%) was added to lift the cells off of the culture well. Microsoft Excel was used to derive representative equations from a graph of % maximum CI vs. time after trypsin addition; these equations were used to calculate the $t_{1/2}$, time to reach 50% of the max CI, for each cell type. The myoferlin-deficient cells showed a 37.9% increase in release time. Cellular adhesion plays a significant role in cell motility, which is a key property in cancer invasion. Thus, the data suggest that myoferlin could play a role in the invasion process.

Introduction

Cancer and the Metastatic Process

It is estimated that over 500,000 Americans lives were lost to cancer and about 1.5 million lives were shaken by a new diagnosis of cancer in 2009 [1]. Cancer is the second most common cause of death in the United States, accounting for approximately one-fourth of all mortalities and only narrowly surpassed by heart disease [1]. Cancer most often becomes deadly when it metastasizes or gains the ability to migrate and invade to other parts of the body. If metastasis could be prevented, cancer could be treated in the local environment and survival rates would likely increase. Cellular adhesion plays a significant role in the metastatic process, shown in Figure 1, because the cancer cells must both overcome their local attachments and form new ones to migrate and invade other tissues. The objective of this study was to develop an assay to measure cellular adhesion *in vitro* and assess the effects of myoferlin depletion on the cellular adhesion.

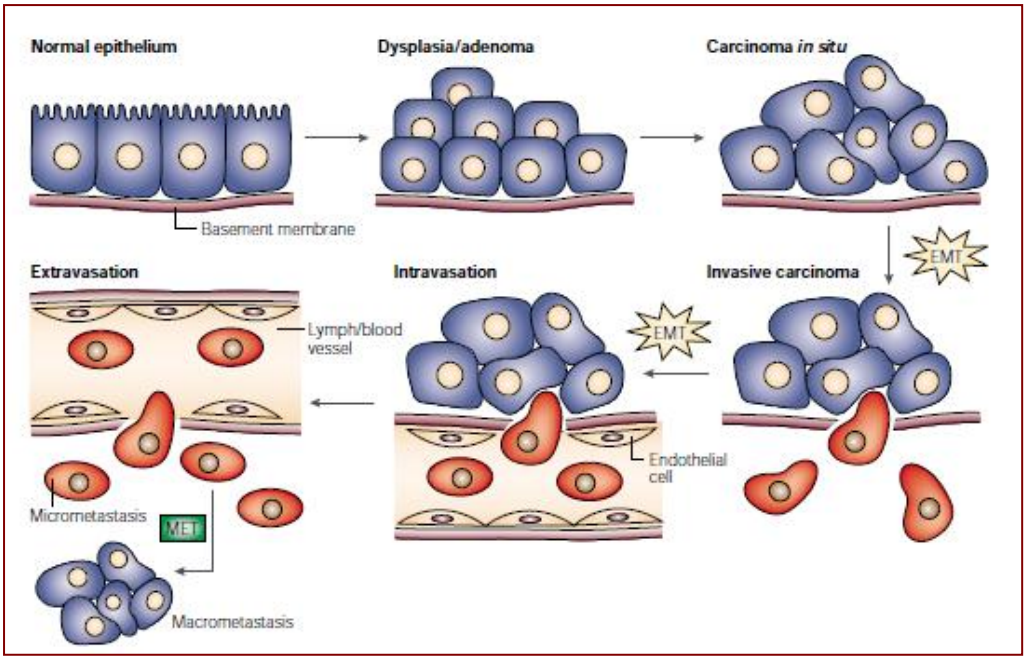

Figure 1: The metastatic process [2]

The Ferlin Protein Family

Myoferlin is part of the mammalian ferlin gene family, which contains six expressed proteins. The ferlin proteins are involved in membrane fusion and maintenance [3,4,5], which is critical for cell motility. Fer-1 was first discovered in *C. elegans*, because it is essential for male fertility [6]. *C. elegans'* sperm do not swim, but crawl. This crawling is similar in manner to the same movement that cancer cells use to migrate to and invade other tissues. Myoferlin is a human homologue of Fer-1 and is over-expressed in invasive breast cancer cells. When the significance in *c. elegans* fertility and over-expression in human cancer are both taken into consideration, myoferlin appears to be a prime candidate for investigation.

Significance

The findings of this project have contributed to the fight against cancer and fields of biology and biomedical engineering as a whole. The unique attribute of cancer research is that because it is focused on abnormal cellular processes, it forces the further understanding of normal cellular processes. Cellular adhesion plays roles in many processes, from cell-to-cell signaling to pathologies such as ALS [7]. Any progress in uncovering the underlying mechanisms of cellular adhesion could contribute to other causes, especially considering that deficiencies or mutations in other ferlin proteins are linked to human pathologies such as deafness and Miyoshi Myopathy [8]. Hence, while this work itself is not disease-curing, it is a contribution towards efforts with possible far-reaching consequences.

Materials and Methods

Cell lines

Experiments used three variations of the MDA-MB-231 human breast cancer cell line. The MDA-MB-231 cell line has been shown to be a metastatic cancer. The three variations used were Wild Type

(WT), Myoferlin Knockdown (KD), and Lentiviral Control (LVC). The WT cells have had no modifications. The KD cells have had the expression of myoferlin completely knocked out using a lentiviral-mediated RNA interference gene silencing [3]. The LVC cells have been exposed to the lentivirus, but with a non-human gene target [3]. The LVC cells serve as a control to account for the presence of the lentivirus itself.

Cell Culture

The cells were grown in two mediums: 1) Dulbecco's Modified Eagle Medium (DMEM) with 10% Fetal Bovine Serum (FBS) and 2) DMEM with 1% FBS. A lower FBS content was needed in order to be able to perform the trypsin release assay; FBS lowers the effectiveness of trypsin. 1% FBS was chosen as the alternative growth medium after running pilot studies with 10% FBS, 1% FBS, 0.5% FBS, 0.1% FBS, 1% Bovine Serum Albumin (BSA), and 0.1% Bovine Serum Albumin. The cells were allowed to attach and grow for 48 hrs and then imaged using phase contrast microscopy, (Figure 6). The factors taken into consideration when judging the quality of the media composition were the similarity of the images to the control (10% FBS) in both number of floating cells and attached cell morphology.

The xCELLigence System (Figure 2) uses an E-plate, which is very similar in appearance to a 96-well cell culture plate, but across the bottom of the wells are gold electrodes [9]. As cells attach to the bottom of the well, the impedance across the electrical circuit increases, which the xCELLigence system monitors and reports as change in Cell Index (CI). CI is a measure of cell number, cell attachment, and cell spreading. Due to this ambiguity in the measurement of CI, the trypsin release assay was incorporated to isolate cell attachment.

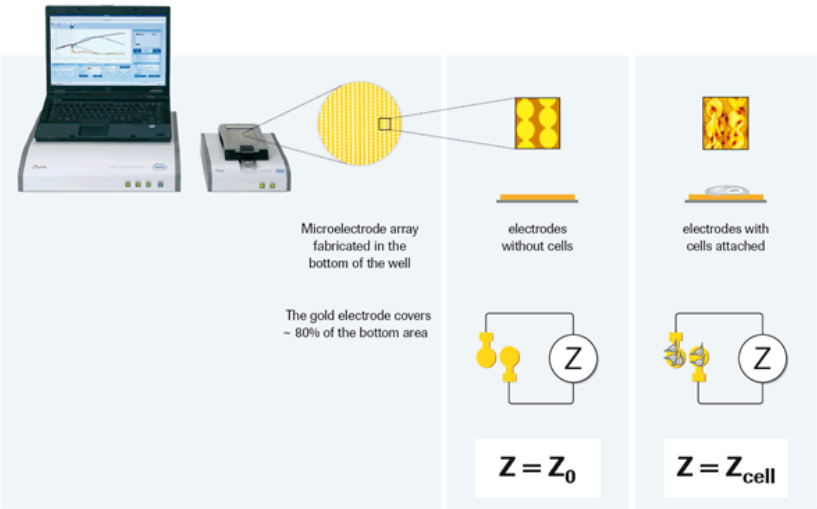

Figure 2: xCELLigence E-plates measure relative impedance and thus relative cellular adhesion, spreading, and number [9]

Before either of the assays could be performed, the cell number needed to be optimized. The optimal cell number had to be low enough that it would be still significantly increasing at 3 hrs, but high enough that it would not be significantly increasing after 48 hrs. Two experiments were performed using $5x10^3$, $1x10^4$, $2x10^4$ and $4x10^4$ cells/well. As can be seen in Figure 3, the $4x10^4$cells/well provided a long period of steadily increasing CI.

Cell Preparation and Seeding

The cells were grown in DMEM 10% FBS culture in T-25 flasks until confluent. They were then lifted with stock trypsin solution (0.5 %) and collected in their final seeding medium (10% or 1% FBS, depending on the trial) and placed into conical tubes. A small (~0.5 mL) sample was set aside for cell counting. The cells were centrifuged at 1200 rpm for 5 min. The remaining media was aspirated and the pellet was re-suspended in the appropriate amount of media to yield a cell density of $4x10^5$ cells/mL.

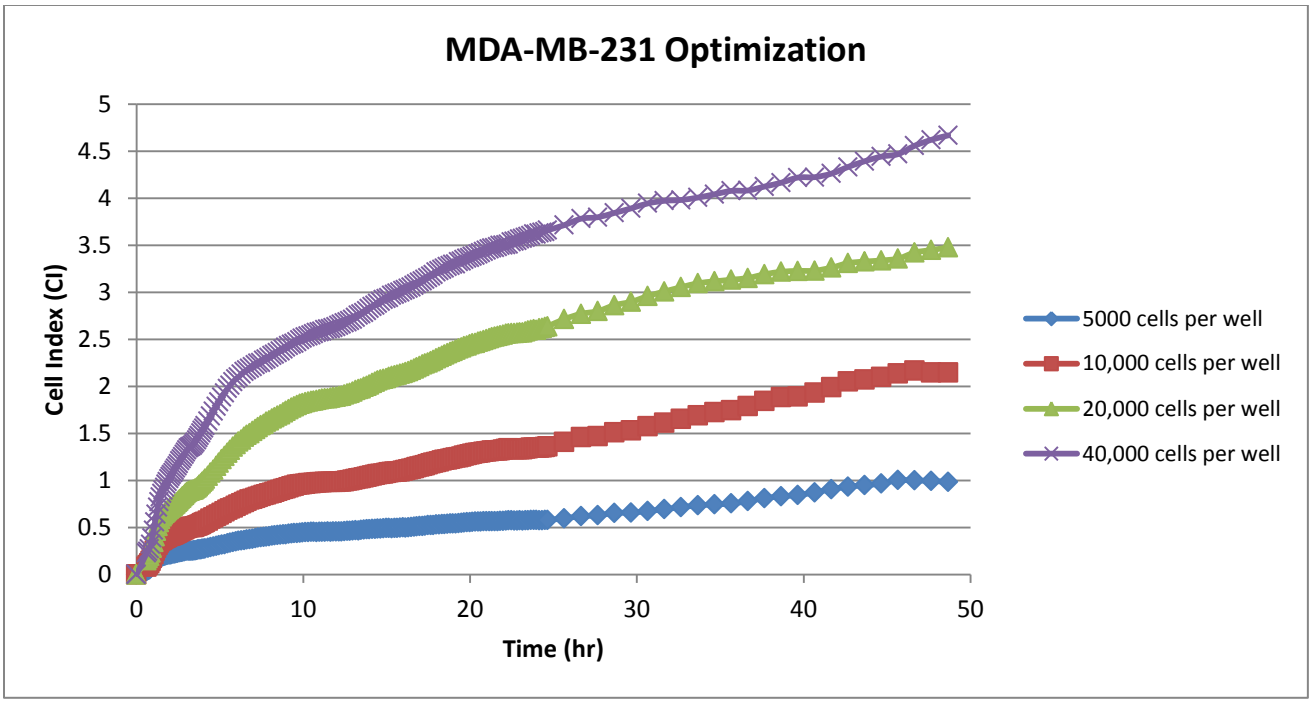

Figure 3: MDA-MB-231 xCELLigence optimization

Media (100µL) was added to each well of the E-plate. The E-plate was placed into the xCELLigence system and a base reading was taken; the xCELLigence system will usethis base reading of impedance as zero when measuring after the cells have been added. 100 µL of the $4x10^5$ cells/mL media mixture were added to the wells in the configuration shown in Table 1. Three plates were run for each type of culture media (1% FBS vs. 10% FBS), resulting in at least 13 replicates for each cell type. The xCELLigence system was set to measure CI according to the schedule shown in Table 2.

Table 1: xCELLigence plating configuration

MDA-MB-231 WT	MDA-MB-231 WT
MDA-MB-231 WT	MDA-MB-231 WT
MDA-MB-231 WT	MDA-MB-231 LVC
MDA-MB-231 LVC	MDA-MB-231 LVC
MDA-MB-231 LVC	MDA-MB-231 LVC
MDA-MB-231 KD	MDA-MB-231 KD
MDA-MB-231 KD	MDA-MB-231 KD
MDA-MB-231 KD	Media

Table 2: xCELLigence schedule

Time Interval	Measurement Rate	Process
0-4 hrs	5 min	Initial Adhesion and Spreading
4-48 hrs	30 min	Further Adhesion and Spreading
48-50 hrs	10 seconds	Trypsin Release Assay (Beginning)
50hrs – END	10 minute	Trypsin Release Assay (End)

Adhesion and Spreading Assay

The relative adhesion and spreading for each well was calculated according to the methods shown in below.

$$Relative\ cell\ adhesion\ and\ spreading\ (RAS) = \frac{(CI\ measurement\ of\ well\ at\ t = 3hrs)}{(Average\ of\ WT\ CI\ values\ at\ t = 3hrs)}$$

The average WT CI value was calculated for each plate and used for the corresponding cell adhesion and spreading calculations. The RAS values for each cell type were combined across all three plates used for

each medium and the standard deviation was evaluated. This data is shown in Figures 6 and 7 in the Results section of this paper.

Trypsin Assay

After 48 hrs, 10µL of 0.41% trypsin at room temperature wer added to each well, yielding a final trypsin concentration of ~0.02%. The cells rounded in appearance. For each well, the CI measured at 48 hrs was set to be 100%. The subsequent CI measurements were converted to a percentage of the maximum CI. The %CI values for each time point were averaged within each cell type for each plate. When plotting the graph of %CI vs time for all plates within a medium type, the result is three curves per cell type, with a total of nine curves, shown in Figures 8 and 9.

Equations

The three data sets for each cell type were used to derive function for each cell type. Due to the shape of the data curves, a first degree exponential decay function ($y = Ae^{-rt}$, A=initial value, r=decay rate) was assumed and the A value was set to 100. The Microsoft Excel Solver Add-in was used to find r. The equation solver compares the function value and the raw data value at each time point and aims to minimize the difference between the two values as well as the entire sum of the differences across all time points. The derived equations were used to calculate the time for a 50% reduction in CI ($t_{1/2}$). These equations and $t_{1/2}$ values are reported in Table 3 in the Results section of this paper. While satisfactory for this project, this model is still preliminary. For future analysis and experiments, a second degree exponential decay is being considered.

Statistical Analysis

All statistical calculations were performed using the software package GraphPad. A normality test was used to determine whether the RAS values in each of the cell types could be assumed to be a normal distribution and thus, validate the use of an ANOVA analysis. An ANOVA analysis compares the

means of two or more data sets and determines whether they are statistically significant ($p<0.0001$). A Tukey test was used to compare all of the possible pairs (WT vs. LVC, WT vs. KD, LVC vs. KD).

Results

Morphology Change

A morphology change was observed in conjunction with the absence of myoferlin, shown in Figure 4. The KD cells take on an epithelioid morphology.

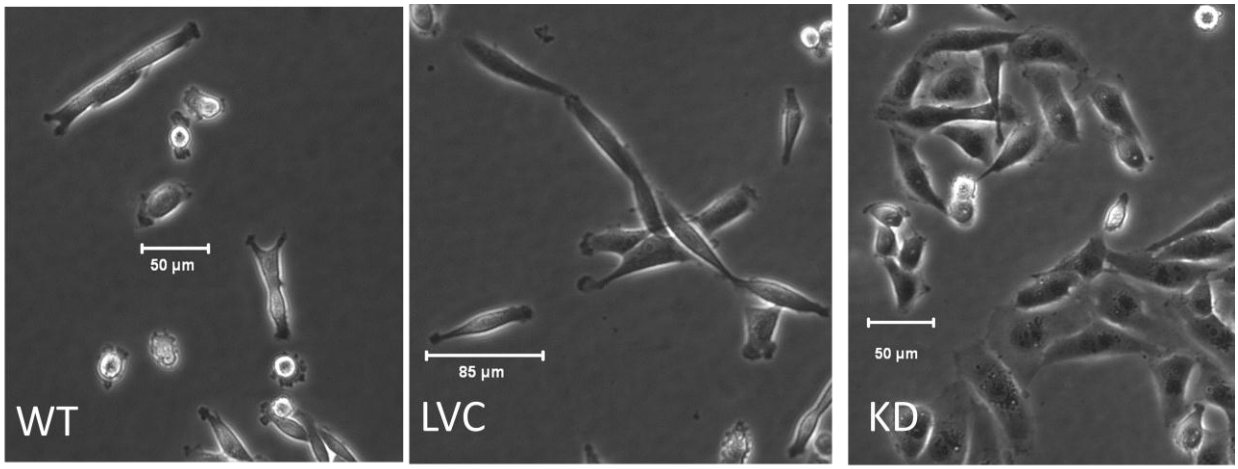

Figure 4: Phase contrast images of the three cell types (20X)

Media Composition Study

In order to perform the trypsin assay, an appropriate lower level of FBS or a FBS substitute had to be used in the medium due to the fact that FBS contains a trypsin inhibitor and thus, neutralizes trysin quickly. Cells were seeded into a 96-well plate, using the same methods as described for the E-plate, and were cultured in the following compositions: 10% FBS, 1% FBS, 0.5% FBS, 0.1% FBS, 1% BSA, and 0.1% BSA. The cells were allowed to attach and grow for 48 hrs, and then imaged using phase contrast microscopy, (Figure 5). The factors taken into consideration when judging the quality of the

media composition were the similarity of the images to the control in both number of floating cells and attached cell morphology.

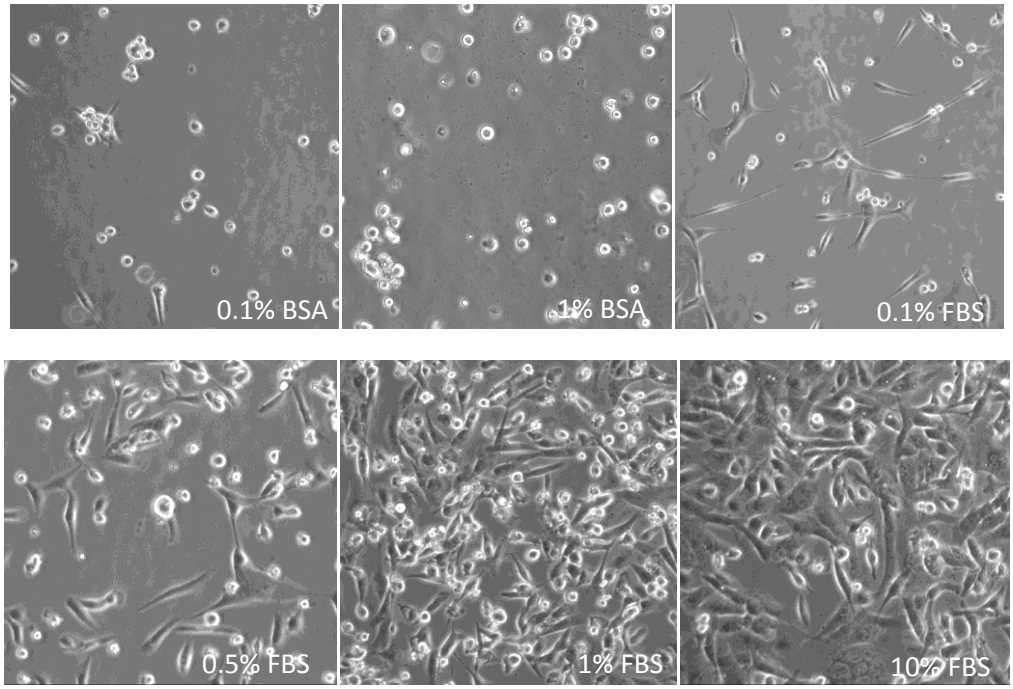

Figure 5: Media Composition Phase Contrast Images (20X)

As shown in Figure 5, all compositions containing BSA were rather dissimilar to the control, with a lot of floating cells and even the attached cells are mostly rounded. Conversely, a low concentration of FBS results in particularly long processes. As evident from the images below, the 1% FBS composition is most similar to the control composition. After ruling out BSA with the images, pilot trypsin experiments were performed. All compositions, with the exception of the control, showed approximately the same amount of rounding in the morphology of the cells, with no major lifting. Thus, the 1% FBS composition was chosen for the trypsin assay.

Adhesion and Spreading Assay

As shown in Figures 6 and 7 below, both media compositions showed a statistically significant difference in adhesion and spreading from the WT and LVC. The KD cells show approximately twice the spreading and adhesion. The only anomaly in this data is that in the 1% FBS media composition, there is a statistical difference between the LVC and WT. However, considering the magnitude of the standard deviation and that the GraphPad software package does not give raw p values, just whether the calculated p value is less than 0.05. Thus, it is not known how close the calculated p value is to 0.05 and this significance could disappear with more experiments.

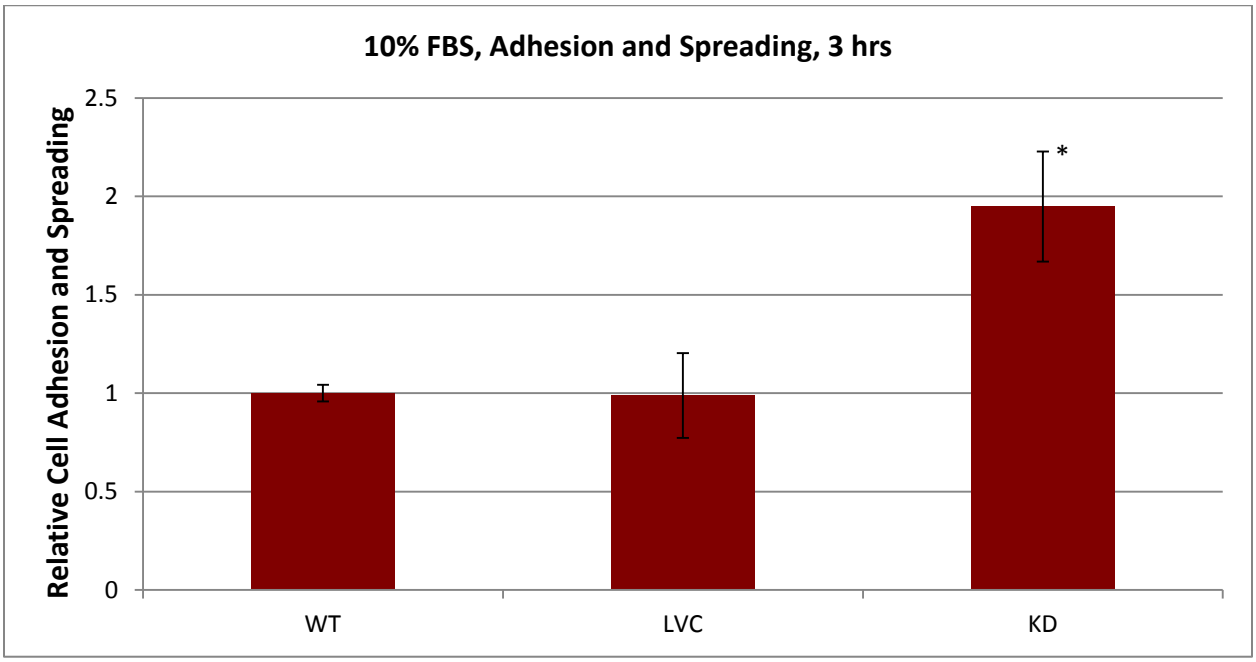

Figure 6: Initial Adhesion and Spreading Assay (10% FBS). *KD is statistically different from the LVC and WT (p<0.0001)

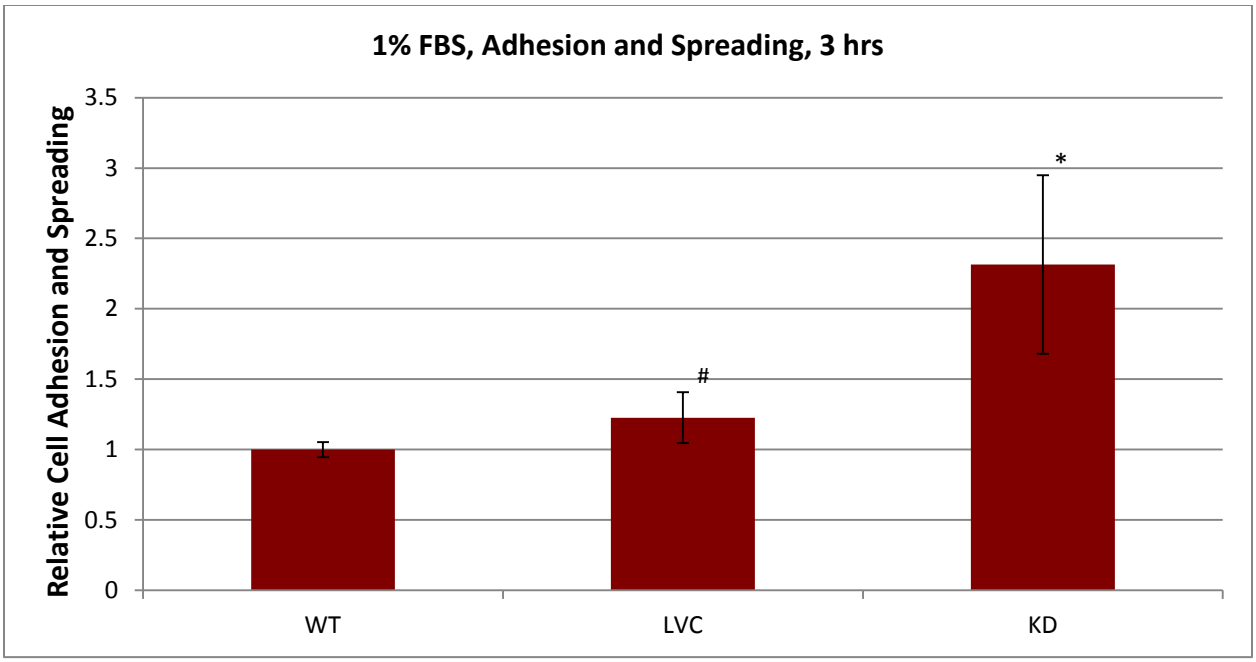

Figure 7: Initial Adhesion and Spreading Assay (1% FBS) *KD is statistically different from WT and LVC ($p<0.001$) #LVC is statistically different from WT ($p<0.05$).

Trypsin Release Assay

As shown in Figure 8, all of the curves have a shape that looks similar to an exponential decay. The zoomed in graph shown in Figure 9 highlights the difference between the KD release curve, which becomes apparent around t=0.5 hrs. The KD cells show a higher percent max CI after ~0.5 hr and, as shown in Table 3, show an increase in $t_{1/2}$ of 37.9%. This reinforces the findings of the initial adhesion and spreading assay that the KD cells had a higher adhesion and spreading. Additional statistical calculations are needed to determine whether this difference is statistically significant.

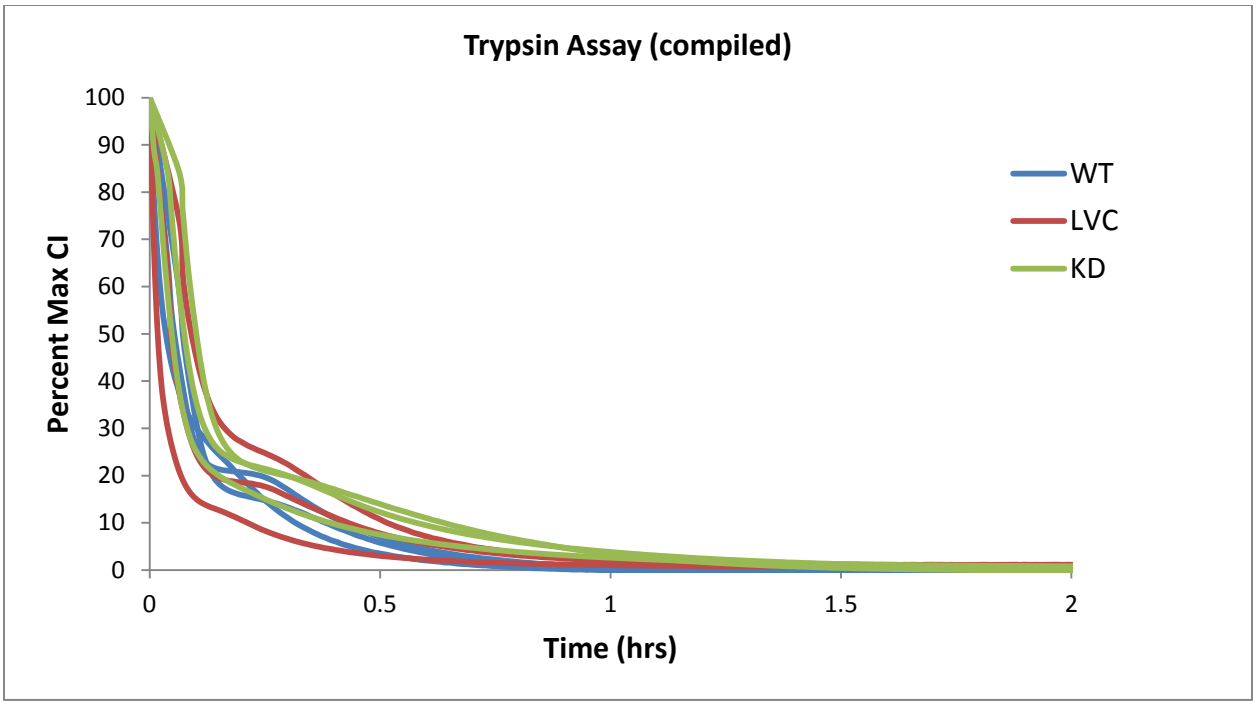

Figure 8: Trypsin Release Assay (1% FBS)

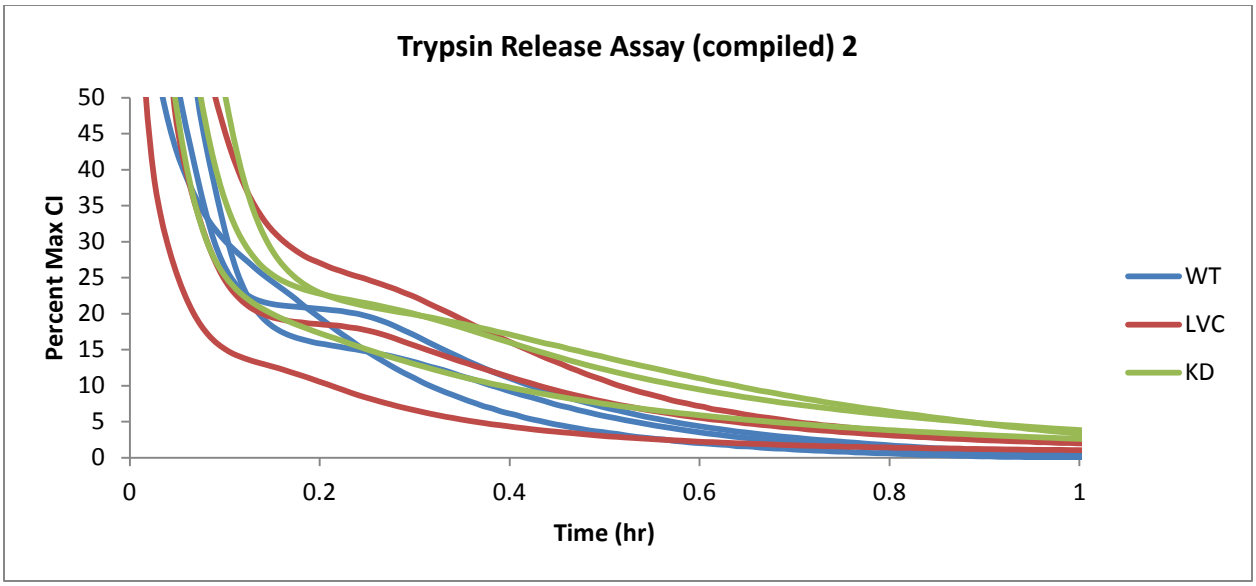

Figure 9: Zoomed-in Trypsin Release Assay (1% FBS)

Table 3: Trypsin Release Assay Calculations

Cell Line	Derived Equation	$t_{1/2}$
WT	$Y=100e^{(-9.716t)}$	~4.28 min
LVC	$Y=100e^{(-10.134t)}$	~4.10 min
KD	$Y=100e^{(-7.20t)}$	~5.78 min

Discussion

From the data above, it is apparent that the depletion of myoferlin has an effect on the cell morphology, spreading, and adhesion. However, the significance of this effect and its interpretation in the broad scale of cancer metastasis remains somewhat unclear. When considering that myoferlin is a human homolog of the *C. elegans*' Fer-1 protein, the morphology change to an epithelioid phenotype seems logical. When *C. elegans* is Fer-1 deficient, a small pseudopod forms, but it is ineffective in spermatozoan motility [4]. It could be hypothesized that a similar mechanism is occurring in myoferlin deficient breast cancer cells.

The data suggest an inverse relationship between cellular motility and adhesion. This relationship seems logical on the premise that in order to migrate, the cell must be able to release from its substrate and overcome cell-cell adhesion as well. Thus, stronger cellular adhesion could result in a lower motility. In fact, other studies with the MDA-MD-231 cells, but different proteins have shown a similar relationship [10,11].

However, other studies, both in breast and other cancers, present data that support the hypothesis of a direct relationship between cell motility and adhesion [12,13]. This hypothesis is also logical, but on the premise that in order to move a cell must be able to form new, stronger attachments to overcome its current ones. This is in line with observed effects in Fer-1 deficient *C. elegans*; the pseudopod can form to a certain extent, but cannot attach effectively. Due to the fact that both arguments are logical, valid and supported by current studies, one can only conclude that there must be a gap of knowledge in the underlying mechanisms and suggest further experiments to close such gaps.

Conclusions and Future Suggestions

Despite the lack of knowledge about the underlying mechanisms at work, solid conclusions can be drawn from the data presented. First of all, the deficiency of myoferlin causes a change in

morphology to an epithelioid phenotype. This is supported by the images shown in Figure 2. In addition to morphology, myoferlin deficiency increases cellular adhesion and spreading. This is supported by both the initial spreading and adhesion assay, which showed an approximate doubling in the KD cells, and the trypsin release assay, which showed a 37.9% increase in $t_{1/2}$ for the KD cells.

For future work, it would be useful to further over-express myoferlin and, hopefully, observe the opposite effect. Furthermore, expansion into other cell lines could provide data on the specific and universal roles of myoferlin in cellular processes. Finally, the effect of myoferlin deficiency on different cellular adhesion processes, such as integrins (cell to ECM) and E-cadherins (cell to cell), could be investigated to further explore the relationship between cellular adhesion and cancer motility and invasion.

Acknowledgements

The author would like to acknowledge The Ohio State University Perinatal Research & Development Fund and The Ohio State University Undergraduate Research Office for their generous funding of this work. Furthermore, the author would like to thank Dr. Douglas Kniss, Dr. Ruth Li, Taryn Summerfield, and Logan Ward for their teaching, guidance, and assistance in the completion of this undergraduate research thesis project.

References

1. American Cancer Society. *Cancer Facts & Figures 2009*. Atlanta: American Cancer Society; 2009.
2. Theiry, Jean Paul. "Epithelial-Mesenchymal Transitions in Tumour Progression." *Nature* 2 (2002): 442-64.
3. Li, Ruth. "The Expression and Effect of Myoferlin Depletion in Breast Cancer Cells." *OSU Knowledge Bank*. The Ohio State University, 2010. Web. 10 May 2011. <http://etd.ohiolink.edu/view.cgi?acc_num=osu1292963348>.
4. Washington, Nicole L., and Samuel Ward. "FER-1 Regulates Ca2+-mediated Membrane Fusion during C. Elegans Spermatogenesis." *Journal of Cell Science* 119 (2006): 2552-562.
5. Demonbreun, Alexis R., Karen A. Lapidos, Konstantina Heretis, Samantha Levin, Rodney Dale, Peter Pytel, Eric C. Svensson, and Elizabeth M. McNally. "5. Myoferlin Regulation by NFAT in Muscle Injury, Regeneration and Repair." *Journal of Cell Science* 123 (2010): 2413-422.
6. Nelson, G. A. "Caenorhabditis Elegans Spermatozoan Locomotion: Amoeboid Movement with Almost No Actin." *The Journal of Cell Biology* 92.1 (1982): 121-31.
7. Bronson, Cynthia. "The Cytoskeleton." 1735 Neil Ave, Columbus, OH. 15 Feb. 2010. Lecture.
8. "The FerlinFamily." *Research Database*. The Jain Foundation. Web. 5 May 2011. <https://www.jain-foundation.org/database/database_ferlin%20family.php>.
9. "Electronic Sensor Technology Applied to Cell Biology." *Roche Applied Science: - XCELLigence System*. Roche Applied Science, 1996. Web. 17 May 2011. <http://www.roche-applied-science.com/sis/xcelligence/index.jsp?&id=xcect_010000>.
10. Xing, Peng, Ji-guang Li, Feng Jin, Ting-ting Zhao, Qun Liu, Hui-ting Dong, and Xiao-lin Wei. "Fascin, an Actin-bundling Protein, Promotes Breast Cancer Progression in Vitro." (2011). *Wiley Database*. Web. 17 May 2011.
11. G. Wen et al., TGFBI expression reduces in vitro and in vivo metastatic potential of lung and breast tumor cells, Cancer Lett. (2011), doi:10.1016/j.canlet.2011.04.010
12. Zhu, Et Al. "EMMPRIN Regulates Cytoskeleton Reorganization And Cell Adhesion in Prostate Cancer." *The Prostate* (2011).
13. McSherry et al.: Breast cancer cell migration is regulated through junctional adhesion molecule-A-mediated activationof Rap1 GTPase. Breast Cancer Research 2011 13:R31.